Supplementary Materials: Photoconduction of Polar and Nonpolar Cuts of Undoped $Sr_{0.61}Ba_{0.39}Nb_2O_6$ Single Crystals

Elke Beyreuther [1]*, Julius Ratzenberger [1], Matthias Roeper [1], Benjamin Kirbus [1], Michael Rüsing [1], Liudmila I. Ivleva [2] and Lukas M. Eng [1,3]

1. Daylight response of z-cut SBN61

In figure S1 the pronounced photosentitivity of SBN already under daylight is illustrated.

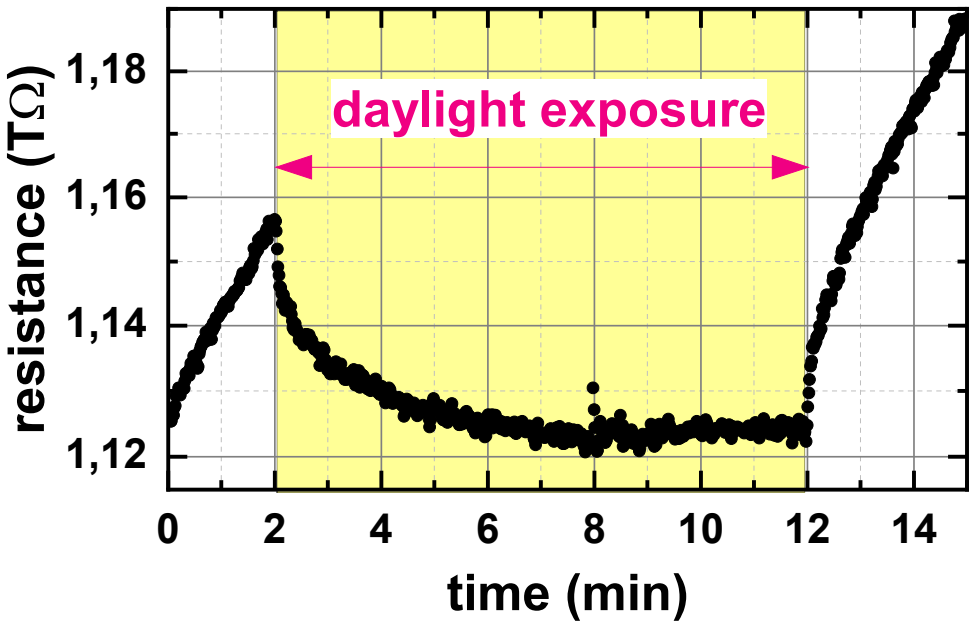

Figure S1. Pronounced photoconductive effect triggered already by diffuse daylight: Resistance vs. time shortly after mounting the z-cut SBN61 crystal in the measurement device. While the sample is shadowed between 0 and 2 minutes and again after 12 minutes, it is exposed to normal laboratory day light between minutes 2 and 12 (indicated by yellowish background). During this period of time a clear resistance decrease occurs. The continuous resistance increase during the shadowed periods is due to slow relaxation of photoinduced charge carriers, as investigated in more detail in the following.

2. Microscopic domain investigations of the polar (z)-cut crystal

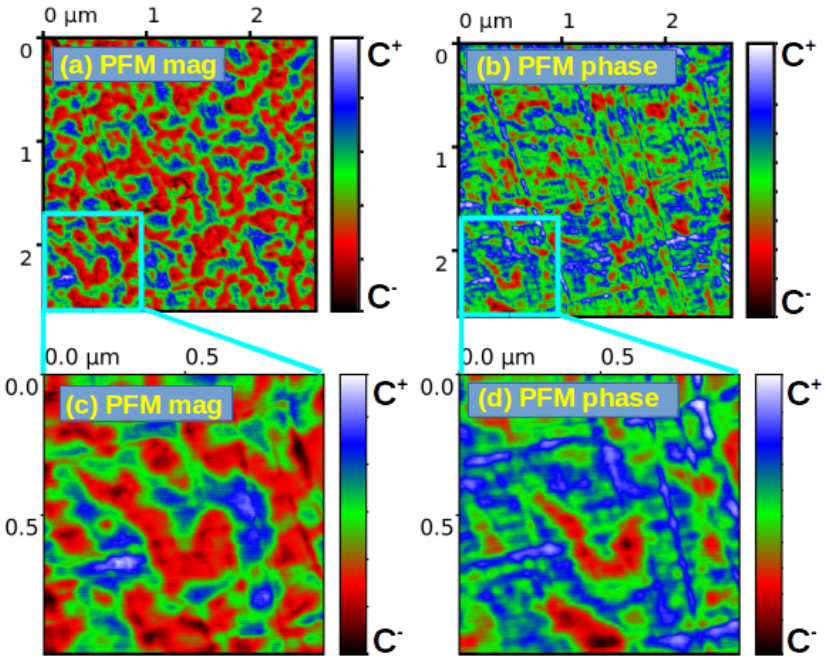

Figure S2. Out-of-plane (a)/(c) amplitude and (b)/(d) phase piezoresponse-force-microscopy (PFM) images of the SBN61 (z-cut) sample showing reproducible natural randomly shaped ferroelectric c+ (red) and c− (blue) domains at different magnifications – images taken with a AIST-NT SmartSPM 1000 system.

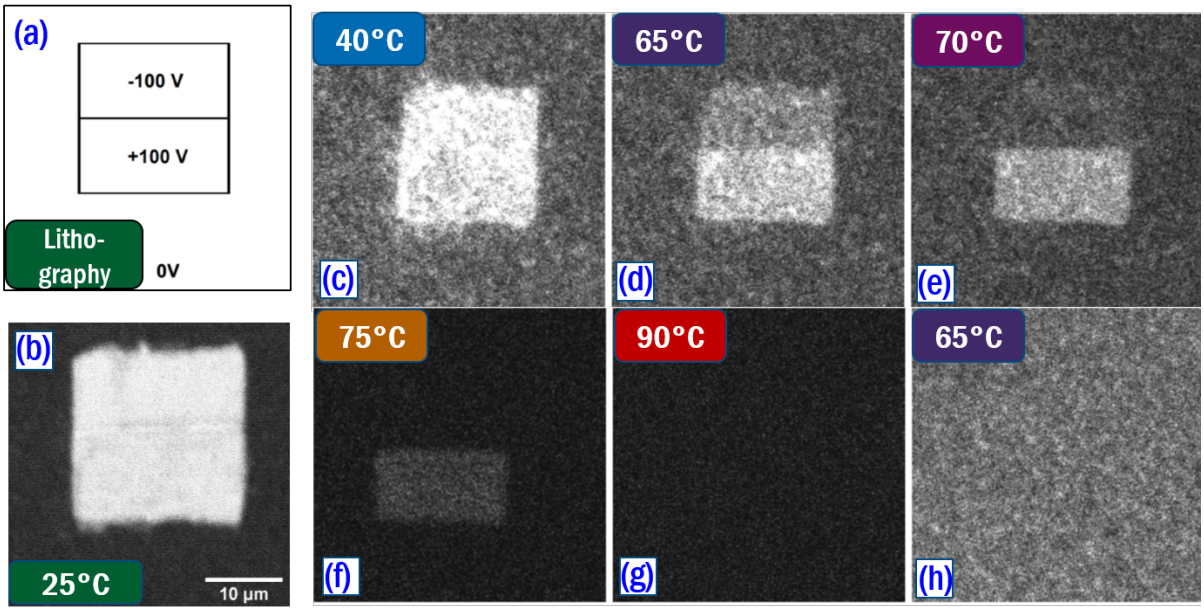

Figure S3. Domain contrast of ferroelectric domains in z-cut SBN61, written by an atomic-force-microscope tip as sketched in panel (a), visualized by Cherenkov second-harmonic-generation microscopy (CSHG, for experimental details refer to [1]) at (b) room temperature and at elevated temperatures (c-h), showing the ferroelectric polarization vanish between 70 and 90 ° C in accordance with the literature.

3. Linear representation of photoconductivity spectra

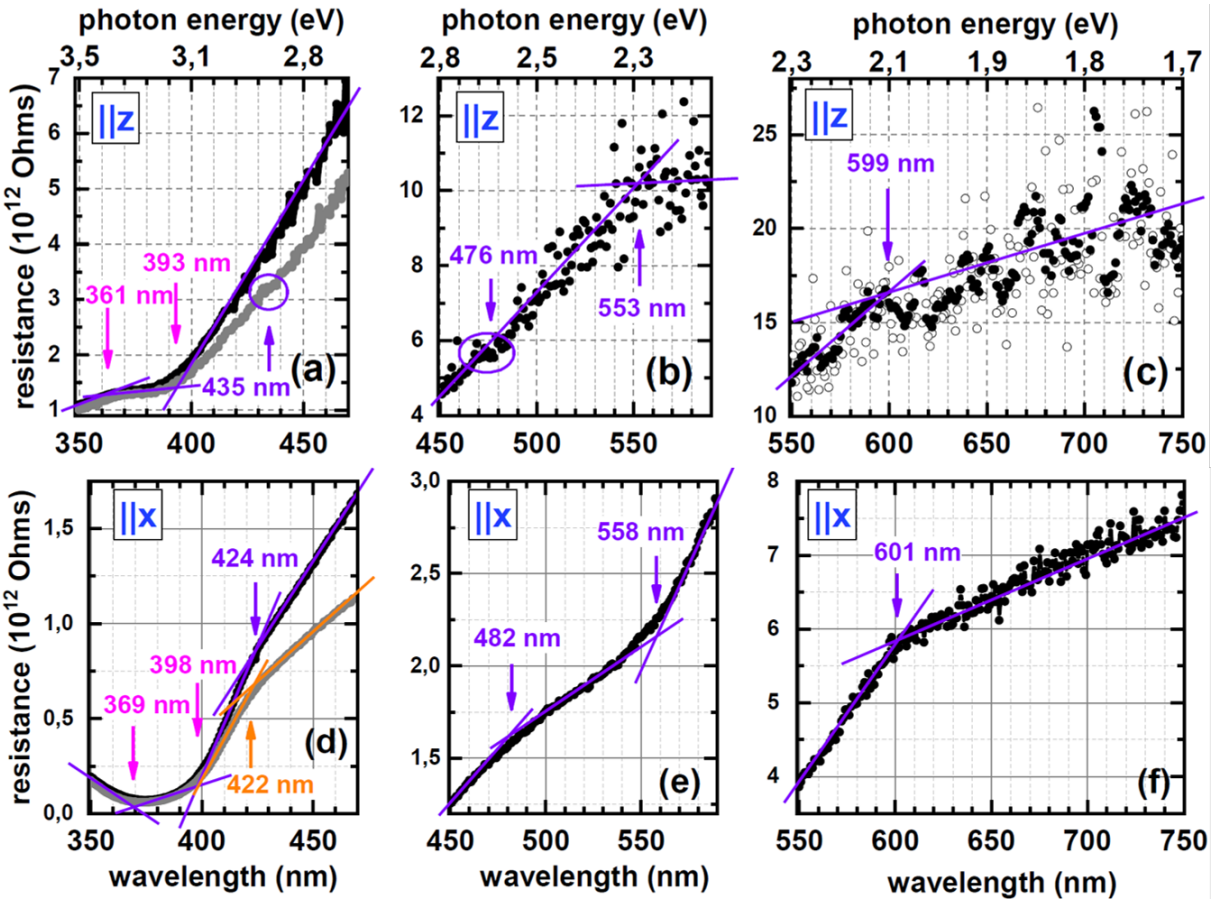

Figure S4. Comparative linear resistance-vs.-wavelength plots with spectral features: While subfigures (a), (b), (c) show the wavelength dependence of the resistance measured along the polar axis (z-cut sample), the subfigures (d), (e), (f) depict the corresponding data recorded for the x-cut sample. The data was acquired within three overlapping partial spectra beginning at the high-wavelength end in all cases. Points of slope change or discontinuities in the from of small plateaus are indicated by arrows. For the subspectra (a) and (d) the two different curves (black vs. grey) demonstrate the degree of reproducibility; for case (c) a smoothed curve (filled circles) is shown alongside with the quite scattering original data (open circles).

4. Light-off transients of the normalized photoconductance

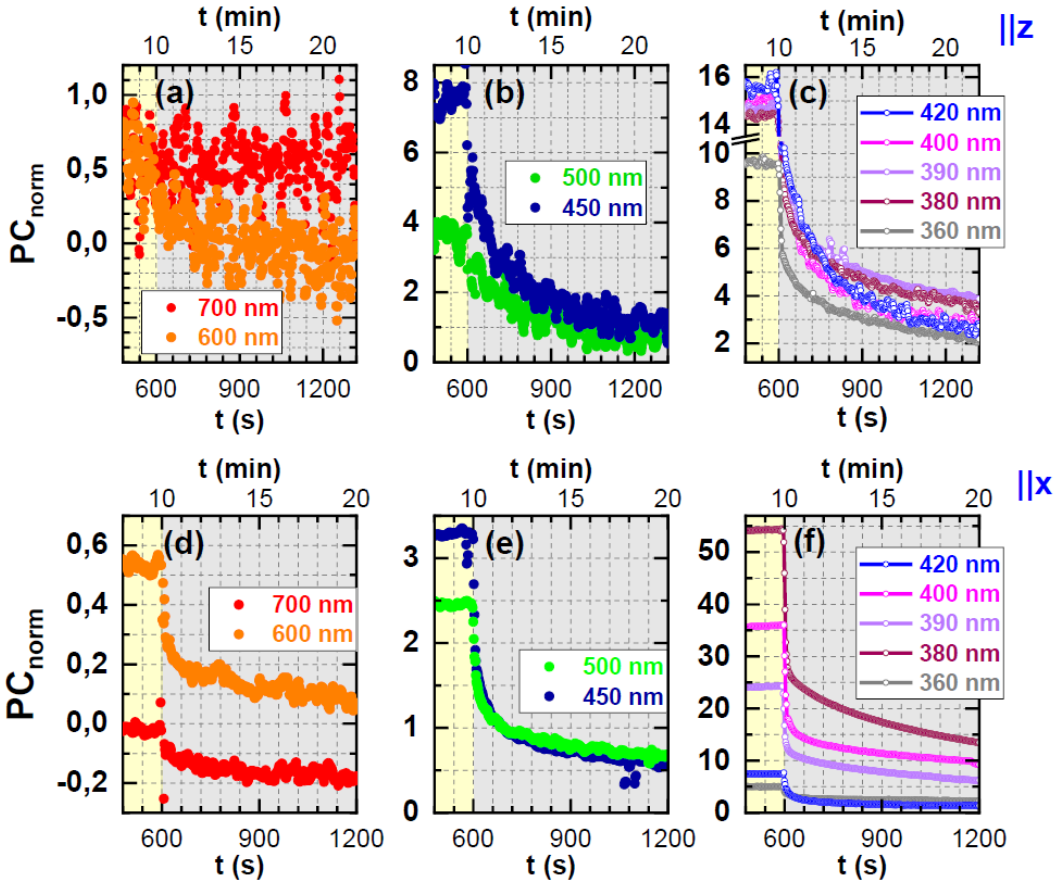

Figure S5. Light-off transients of the [(a)-(c)] z-cut and [(d)-(f)] the x-cut SBN61 sample for selected wavelengths, showing the first 10 minutes after switching off a 60-min illumination interval (having been illustrated in the two previous Figures 4 and 5 of the main text). Greyish background indicates darkness and yellowish background indicates illumination. Note that, for some of the curves, at longer wavelengths (600 nm, 700 nm) an artifact, namely a drift of the dark resistance R_0 due to a kind of electroresistive effect of the measuring voltage, mimics negative PC values within both the light-on and the light-off transients.

5. Dark current-voltage characteristics of z-cut SBN61

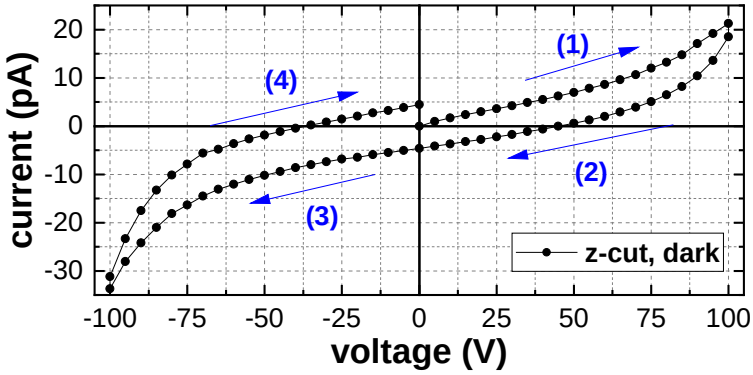

Figure S6. Current-voltage characteristics of the z-cut SBN61 polydomain crystal in the dark up to ±100 V, measured along the polar z-axis with arrows and numbers in brackets indicating the order and direction of the applied voltage ramps. As expected, a hysteretic ohmic behavior is measured.

References

1. B. Kirbus, C. Godau, L. Wehmeier, H. Beccard, E. Beyreuther, A. Haussmann, and L. M. Eng, T. Real-Time 3D Imaging of Nanoscale Ferroelectric Domain Wall Dynamics in Lithium Niobate Single Crystals under Electric Stimuli: Implications for Domain-Wall-Based Nanoelectronic Devices. *ACS Appl. Nano Mater.* **2019**, 2(9), 5787-5794. https://doi.org/10.1021/acsanm.9b01240